Article

# Interaction between the Type-3 Copper Protein Tyrosinase and the Substrate Analogue *p*-Nitrophenol Studied by NMR

Armand W. J. W. Tepper, Luigi Bubacco, and Gerard W. Canters

*J. Am. Chem. Soc.*, **2005**, 127 (2), 567-575• DOI: 10.1021/ja0454687 • Publication Date (Web): 23 December 2004



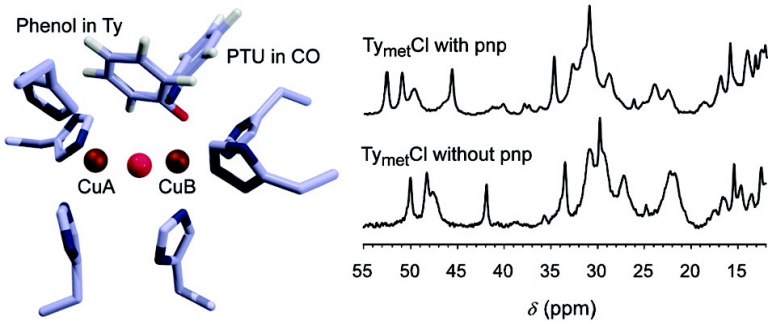


## More About This Article

Additional resources and features associated with this article are available within the HTML version:

- Supporting Information
- Links to the 1 articles that cite this article, as of the time of this article download
- Access to high resolution figures
- Links to articles and content related to this article
- Copyright permission to reproduce figures and/or text from this article

View the Full Text HTML

J|A|C|S
ARTICLES
Published on Web 12/23/2004

# Interaction between the Type-3 Copper Protein Tyrosinase and the Substrate Analogue *p*-Nitrophenol Studied by NMR

Armand W. J. W. Tepper,[†] Luigi Bubacco,[‡] and Gerard W. Canters*,[†]

*Contribution from the Leiden Institute of Chemistry, Gorlaeus Laboratories, Leiden University, Einsteinweg 55, 2333 CC, Leiden, The Netherlands, and the Department of Biology, University of Padua, Via Trieste 75, 30121 Padua, Italy*

Received July 28, 2004; E-mail: canters@chem.leidenuniv.nl

***Abstract:*** The interaction of the monooxygenating type-3 copper enzyme Tyrosinase (Ty) from *Streptomyces antibioticus* with its inhibitor *p*-nitrophenol (pnp) was studied by paramagnetic NMR methods. The pnp binds to oxidized Ty ($Ty_{met}$) and its halide ($F^-$, $Cl^-$) bound derivatives with a dissociation constant in the mM range. The $Cu_2$ bridging halide ion is not displaced upon the binding of pnp showing that the pnp does not occupy the $Cu_2$ bridging position. The binding of pnp to $Ty_{met}$ or $Ty_{met}Cl$ leads to localized changes in the type-3 $(Cu-His_3)_2$ coordination geometry reflecting a change in the coordination of a single His residue that, still, remains coordinated to Cu. The binding of pnp to $Ty_{met}Cl$ causes a decrease in the $Cu_2$ magnetic exchange parameter $-2J$ from 200 $cm^{-1}$ in the absence to 150 $\pm$ 10 $cm^{-1}$ in the presence of pnp. From the $^1H$ and $^2D$ NMR relaxation parameters of pnp bound to $Ty_{met}$, a structural model of pnp coordination to the Ty type-3 center could be derived. The model explains the absence of hydroxylase activity in the closely related type-3 copper protein catechol oxidase. The relevance of the experimental findings toward the Ty catalytic mechanism is discussed.

## Introduction

Tyrosinase (Ty) catalyzes the ortho hydroxylation of monophenolic substrates (monophenolase activity) and the subsequent oxidation of the diphenolic products to the quinone analogues (diphenolase activity). The reactions are rate limiting in the biosynthesis of melanin pigments, that fulfill various roles in different organisms.[1] The enzyme is widely distributed throughout the phylogenetic scale and occurs in organisms ranging from bacteria to man. In mammals, Ty is responsible for skin and hair pigmentation and defects in the enzyme are related to a range of medical conditions such as type I human oculocutaneous albinism.[2] In fruits and mushrooms, the enzyme is responsible for the economically undesirable browning that occurs upon bruising or long-term storage, while in plant products such as cocoa, raisins and green tea, the action of Ty gives rise to distinct organoleptic properties.[3] The enzyme has further been reported to catalyze the dehalogenation of xenobiotic fluorophenols,[4] a reaction potentially applicable in bioremediation. Consequently, the enzyme poses considerable interest from medical, agricultural, and industrial points-of-view.

Ty is a member of the type-3 copper protein family, that further includes the hemocyanins (Hcs) and the catechol oxidases (COs). The type-3 copper proteins are thought to have developed from an ancient ancestor that was possibly involved in scavenging of (toxic) oxygen in a predominantly anaerobic atmosphere.[5] The type-3 proteins contain a binuclear copper active site that is comprised of two closely spaced copper atoms each coordinated by 3 histidine residues. Although the dinuclear site is highly conserved as witnessed by its characteristic spectroscopic signatures, by sequence homologies and by the available crystal structures for several Hcs[6−9] and CO,[10] the functionality of the Tys, Hcs, and COs is different. While Hcs function as oxygen carriers and oxygen storage proteins in arthropods and molluscs, the COs oxidize diphenols to the corresponding quinones but lack the Ty hydroxylation activity.

The Ty type-3 site can exist in four forms. The (*a*) reduced [Cu(I) Cu(I)] species ($Ty_{red}$) binds molecular oxygen to render the (*b*) oxygenated [Cu(II)$-O_2^{2-}-$Cu(II)] species ($Ty_{oxy}$), in which molecular oxygen is bound to the $Cu_2$ center as peroxide in a $\mu$-$\eta^2$:$\eta^2$ side-on bridging mode.[11] The $Ty_{oxy}$ form is competent to react with monophenols and diphenols and is characterized by a strong Ligand to Metal Charge Transfer (LMCT) band centered around 345 nm. Upon reaction of $Ty_{oxy}$ with mono- or diphenolic substrates, the (*c*) oxidized [Cu(II)−

[†] Leiden University.
[‡] University of Padua.

(1) van Gelder, C. W.; Flurkey, W. H.; Wichers, H. J. *Phytochemistry* **1997**, *45*, 1309−1323.
(2) Oetting, W. S. *Pigment Cell Res.* **2000**, *13*, 320−325.
(3) Seo, S. Y.; Sharma, V. K.; Sharma, N. *J. Agric. Food Chem.* **2003**, *51*, 2837−2853.
(4) Battaini, G.; Monzani, E.; Casella, L.; Lonardi, E.; Tepper, A. W.; Canters, G. W.; Bubacco, L. *J. Biol. Chem.* **2002**, *277*, 44606−44612.
(5) van Holde, K. E.; Miller, K. I.; Decker, H. *J. Biol. Chem.* **2001**, *276*, 15563−15566.
(6) Cuff, M. E.; Miller, K. I.; van Holde, K. E.; Hendrickson, W. A. *J. Mol. Biol.* **1998**, *278*, 855−870.
(7) Magnus, K. A.; Hazes, B.; Ton-That, H.; Bonaventura, C.; Bonaventura, J.; Hol, W. G. *Proteins* **1994**, *19*, 302−309.
(8) Perbandt, M.; Guthohrlein, E. W.; Rypniewski, W.; Idakieva, K.; Stoeva, S.; Voelter, W.; Genov, N.; Betzel, C. *Biochemistry* **2003**, *42*, 6341−6346.
(9) Volbeda, A.; Hol, W. G. *J. Mol. Biol.* **1989**, *209*, 249−279.
(10) Klabunde, T.; Eicken, C.; Sacchettini, J. C.; Krebs, B. *Nat. Struct. Biol.* **1998**, *5*, 1084−1090.
(11) Solomon, E. I.; Sundaram, U. M.; Machonkin, T. E. *Chem. Rev.* **1996**, *96*, 2563−2605.

$OH^--Cu(II)$] met species ($Ty_{met}$) is formed, which is competent to react with diphenols only. The $Ty_{met}$ form is the predominant species in the absence of substrate and can bind a range of organic and inorganic ligands that yield complexes in which the enzymatic activity is inhibited.[12−15] The Cu(II) ions in native $Ty_{met}$ are bridged by a hydroxide ion that can be replaced by a halide ion ($X^- = F^-$, $Cl^-$, $Br^-$),[13,14] and they are antiferromagnetically coupled to yield a diamagnetic ground-state. Finally, (*d*) a half-oxidized [Cu(I) $OH^-$-Cu(II)] species ($Ty_{half-met}$) can be prepared in which only one of the two coppers occurs in the oxidized form, which is, thus, EPR active.

The interaction of $Ty_{met}$ with exogenous ligands is difficult to probe due to the scarcity of suitable spectroscopic methods. The $Ty_{met}$ enzyme is devoid of strong transitions in the UV/Vis and cannot be studied by EPR methods. However, it has been shown that the $Ty_{met}$ paramagnetic triplet state is partially populated at room temperature, rendering the site amenable to paramagnetic NMR study.[16] Although paramagnetic NMR is usually not feasible for copper systems due to the inherently large widths of the NMR signals, $Ty_{met}$, a Cu-substituted aminopeptidase,[17] and some antiferromagnetically coupled dinuclear Cu(II) complexes (e.g., refs 18−20) appear to give remarkably sharp paramagnetically shifted NMR signals due to fast electronic relaxation.[16,21]

Since the paramagnetism is only sensed by the protons close to the metallic center, paramagnetic NMR provides a powerful and selective probe of the coordination geometry of the active site and the changes that occur upon ligand binding.[22] The method has previously been used to study inhibitor binding to $Ty_{met}$.[12,13] It was also demonstrated that *S. antibitioticus* Ty contains a classical type-3 site in which the two copper ions are coordinated by six histidine residues through their $N^\epsilon$ atoms,[16] as in the Hcs and COs.

Although the mechanism of the enzyme has been addressed by a wide variety of (bio)chemical, spectroscopic, and theoretical methods, its structural details remain obscure to date. The crucial and rate-limiting step in the rather complex kinetic mechanism[23] is the $Ty_{oxy}$ catalyzed hydroxylation reaction that comprises fissure of the peroxide O−O bond and oxygen transfer to the bound phenolic substrate and for which various mechanisms have been proposed (reviewed in, e.g., refs 24−26).

A critical event is the binding of phenolic substrate to $Ty_{oxy}$. It is generally assumed that phenolate coordinates axially to one of the copper atoms in the Ty active site but experimental evidence for this is scarce. The binding of the phenol is further thought to activate the bound peroxide.[11] Due to their transient nature, the complexes of Ty with monophenols are difficult to study. However, with *p*-nitrophenol (pnp), the presence of the strongly electron withdrawing nitro group sufficiently deactivates the phenolic ring to prevent its hydroxylation. In fact, pnp acts as a simple competitive inhibitor in the conversion of L-DOPA with an inhibition constant in the mM range.[27]

Here, we report on a paramagnetic NMR study of the interaction of pnp with $Ty_{met}$ and its fluoride and chloride bound derivatives, which is aimed at providing insight into the binding mode of monophenols to the Ty active site. The results have a direct bearing on the understanding of the substrate inhibition in the monophenolase reaction and they provide further insight into the hydroxylation mechanism in the monophenolase reaction.

## Materials and Methods

**A. Protein Isolation and Purification.** The enzyme was obtained from the growth medium of liquid cultures of *Streptomyces antibioticus* harboring the pIJ703 Ty expression plasmid.[12] The protein was purified according to published procedures.[12] Purity was checked by SDS-PAGE and exceeded 95% in all preparations. Protein concentrations in pure samples were determined optically using a value of 82 $mM^{-1}cm^{-1}$ for the extinction coefficient at 280 nm.[28] The protein was stored at −80 °C at a concentration of 1 mg/mL in 100 mM Pi buffer at pH 6.8 containing 20% glycerol as a cryoprotectant. Prior to further experiments, glycerol was removed from the storage buffer by repetitive dilution and concentration by using Amicon ultra-filtration over a 10 kDa cutoff membrane.

**B. Paramagnetic $^1$H NMR Measurements.** NMR $Ty_{met}$ samples (∼0.6 mM in 100 mM NaPi at pH 6.80) were prepared as described before[16] and contained 5% $D_2O$ for the lock signal. In standard titration experiments, the [pnp] was varied by stepwise addition of $\mu$L amounts of a 20 mM pnp stock solution made up in the NMR buffer. $^1$H spectra were recorded at 600 and 300 MHz and at 4 °C using a Bruker DMX-600 or DPX-300 spectrometer with the application of a $180°-\tau-90°-t_A$ super-WEFT pulse sequence,[29] an interpulse delay time of typically 55 ms and a 8 $s^{-1}$ repetition rate. Depending on the required signal-to-noise ratio, 4000 to 64 000 free induction decays were recorded and Fourier transformed using exponential apodization and a 40−60 Hz line-broadening function to increase the signal-to-noise ratio. The spectra were baseline corrected in the program Mestre-C (Cobas, J. C., Cruces, J., and Sardina, F. J., Universidad de Santiago de Compostela, Spain) using its spline based semiautomatic fitting procedure. All spectra were calibrated on the water signal.

**C. NMR Measurements of the Bulk pnp Signals.** The NMR shift and relaxation parameters of a free ligand in the bulk solution contain information on the ligand bound to the (paramagnetic) protein, provided that the ligand exchange between the free and the protein-bound states is sufficiently fast.[30] The equations for the observed paramagnetic contributions to the chemical shift and the transversal and longitudinal relaxation rates (for all exchange conditions) are given by[22]


(12) Bubacco, L.; Vijgenboom, E.; Gobin, C.; Tepper, A. W. J. W.; Salgado, J.; Canters, G. W. *J. Mol. Catal. B: Enzymol.* **2000**, *8*, 27−35.
(13) Tepper, A. W.; Bubacco, L.; Canters, G. W. *J. Biol. Chem.* **2002**, *277*, 30436−30444.
(14) Tepper, A. W.; Bubacco, L.; Canters, G. W. *J. Biol. Chem.* **2003**, *279*, 13425−13435.
(15) Wilcox, D. E.; Porras, A. G.; Hwang, Y. T.; Lerch, K.; Winkler, M. E.; Solomon, E. I. *J. Am. Chem. Soc.* **1985**, *107*, 4015.
(16) Bubacco, L.; Salgado, J.; Tepper, A. W.; Vijgenboom, E.; Canters, G. W. *FEBS Lett.* **1999**, *442*, 215−220.
(17) Holz, R. C.; Bennett, B.; Chen, G. C.; Ming, L.-J. *J. Am. Chem. Soc.* **1998**, *120*, 6329−6335. Lin, L. Y.; Park, H. I.; Ming, L. J. *J. Biol. Inorg. Chem.* **1997**, *2*, 744−749.
(18) Asokan, A.; Manoharan, P. T. *Inorg. Chem.* **1999**, *38*, 5642−6554.
(19) Brink, J. M.; Rose, R. A.; Holz, R. C. *Inorg. Chem.* **1996**, *35*, 2878−2885.
(20) Murthy, N. N.; Karlin, K. D.; Bertini, I.; Luchinat, C. *J. Am. Chem. Soc.* **1997**, *119*, 2156−2162.
(21) Clementi, V.; Luchinat, C. *Acc. Chem. Res.* **1997**, *31*, 3351−361.
(22) Bertini, I.; Luchinat, C. *Coord. Chem. Rev.* **1996**, *150*. LaMar, G. N., Horrocks, W. deW., Holm, R. H. *NMR of Paramagnetic Molecules*; Academic Press: London, 1973.
(23) Sanchez-Ferrer, A.; Rodriguez-Lopez, J. N.; Garcia-Canovas, F.; Garcia-Carmona, F. *Biochim. Biophys. Acta* **1995**, *1247*, 1−11.
(24) Karlin, K. D.; Tyeklár, Z. *Bioinorganic Chemistry of Copper*; Chapman & Hall: New York, 1993.
(25) Solomon, E. I.; Chen, P.; Metz, M.; Lee, S.-K.; Palmer, A. E. *Angew. Chem., Int. Ed.* **2001**, *40*, 4570−4590.
(26) Lewis, E. A.; Tolman, W. B. *Chem. Rev.* **2004**, *104*, 1047−1076.
(27) Conrad, J. S.; Dawso, S. R.; Hubbard, E. R.; Meyers, T. E.; Strothkamp, K. G. *Biochemistry* **1994**, *33*, 5739−5744.
(28) Jackman, M. P.; Hajnal, A.; Lerch, K. *Biochem. J.* **1991**, *274* (Pt 3), 707−713.
(29) Inubushi, T.; Becker, E. D. *J. Magn. Reson.* **1983**, *51*, 128−133.
(30) Swift, T. J. In *NMR of Paramagnetic Molecules*; La Mar, G. N., Horrocks, W., Jr., Holm, R. H., Eds.; Academic Press: London, 1973; pp 53−83.

$$\Delta\omega_p = \frac{f_M}{{\tau_M}^2}\frac{\Delta\omega_M}{(R_{2M}+\tau_M^{-1})^2+\Delta{\omega_M}^2} = f_M{\Delta\omega_M}^{app} \quad (1)$$

$$R_{2p} = \frac{f_M}{\tau_M}\frac{{R_{2M}}^2+R_{2M}\tau_M^{-1}+\Delta{\omega_M}^2}{(R_{2M}+\tau_M^{-1})^2+\Delta{\omega_M}^2} = f_M{R_{2M}}^{app} \quad (2)$$

$$R_{1p} = f_M(T_{1M}+\tau_M)^{-1} = f_M{R_{1M}}^{app} \quad (3)$$

where $\Delta\omega_p$, $R_{2p}$ ($= {T_{2p}}^{-1}$) and $R_{1p}$ ($= {T_{1p}}^{-1}$) are the paramagnetic contributions to the shift (in rad·s$^{-1}$), the $R_2$ (in Hz) and the $R_1$ (in Hz) of the bulk ligand, respectively, and $\Delta\omega_M$, $R_{2M}$, and $R_{1M}$ are the corresponding parameters for the ligand bound to the protein. $f_M$ denotes the molar fraction of ligand bound at the paramagnetic center and $\tau_M$ is the lifetime of the ligand in the metal-bound state. When a solution of Ty is titrated with a solution of pnp, both the pnp and Ty concentrations change during the experiment. To facilitate interpretation of the data it is convenient to express $f_M$ in terms of $R$, defined as the ratio between the total pnp and Ty concentrations, as given by eq 4

$${f_M}^{-1} = R + \frac{K_d R}{pnp_0} + \frac{K_d}{Ty_0} \quad (4)$$

The latter equation is valid provided that $R \gg 1$. $Ty_0$ represents the [$Ty_{met}$] at the start of the experiment and $pnp_0$ represents the [pnp] in the added stock solution.

The measurements were performed using either $^1$H or $^2$D NMR. While the absolute shifts (in ppm) of the two pnp signals in the fully $Ty_{met}$ bound form are the same for $^1$H and $^2$D pnp, the $\Delta\omega_M$ in eqs 1 and 2 is proportional to the gyromagnetic ratio of the nucleus under investigation and, as a consequence, the $^2$D $\Delta\omega_M$ amounts to 0.152 the $^1$H $\Delta\omega_M$. When $R_{2M} < \Delta\omega_M$ and $\tau_M^{-1} \ll \Delta\omega_M$ (slow exchange), eq 1 simplifies to $\Delta\omega_p \approx f_M/{\tau_M}^2\Delta\omega_M$. This means that the shifts of the bulk pnp signals for the protonated and deuterated pnp obey the relation $\Delta{\omega_M}^H/\Delta{\omega_M}^D = \Delta{\omega_p}^D/\Delta{\omega_p}^H$. Therefore, toward the slow exchange limit, the observed $^2$D shift measured in ppm amounts to 44 times the $^1$H shift. For fast exchange ($\tau_M^{-1} \gg \Delta\omega_M$), on the other hand, equal shifts (in ppm) are expected for both $^1$H and $^2$D. As for the relaxation rates, the paramagnetic $R_{2M}$ scales with the square of the nuclear gyromagnetic ratio, meaning that the $^2$D $T_{2M}$ should be 44 times that of the $^1$H $T_{2M}$. An evaluation of the $^2$D ${T_{2M}}^{app}$ values, however, should also include the quadrupolar relaxation contribution that depends on the rotational correlation time $\tau_R$ and may dominate the $T_2$ when the ligand is bound to a protein with slow molecular tumbling.

$T_1$ values of $^1$H pnp were measured by standard inversion recovery using at least 16 values for the interpulse delay time. After baseline correction, signal intensities were measured using peak areas. The $R_2$ values of the pnp $^1$H or $^2$D signals were determined from the resonance line-widths by line-shape simulation using the line fitting module in the Mestre-C program. The obtained line-widths were corrected for the contribution introduced by the LB function, after which the $R_2$ values were calculated from the relation $R_2 = \pi\Delta\upsilon$ where $\Delta\upsilon$ denotes the line-width at half-height. The $T_1$, $R_2$, and signal shifts of the bulk pnp signals were corrected for the diamagnetic contribution, the latter being obtained by measuring the $T_1$, $R_2$, and shift of the pnp bulk signals after reducing paramagnetic $Ty_{met}$ to diamagnetic $Ty_{red}$ with excess hydroxylamine [13] at the end of the titration experiment.

## Results

**A. Titrations of Native $Ty_{met}$, $Ty_{met}F$, and $Ty_{met}Cl$ with *p*-Nitrophenol Followed by Paramagnetic $^1$H NMR. 1. Titration of Native $Ty_{met}$.** The paramagnetic $^1$H NMR spectrum of native $Ty_{met}$ is characterized by several broad and partially overlapping signals between 50 and 13 ppm, which integrate to a signal intensity of 18 ± 2 protons accounting for six coordinating His residues, each contributing three protons. Figure 1A shows $^1$H paramagnetic NMR spectra of a sample of 0.7 mM of the native $Ty_{met}$ enzyme in the presence of increasing amounts of pnp from 0 to 1.77 mM at 4 °C and pH 6.8. As the [pnp] is increased, signals *a* and *c* appear to shift toward signal *b* at ~30 ppm, which is accompanied by severe line-broadening, while the remainder of the spectrum is much less sensitive to the presence of pnp. Signal *c* was previously assigned to a solvent exchangeable His N$^\delta$ proton while signal *b* was attributed to two overlapping His C$^\delta$/C$^\epsilon$ proton signals. The similarity in the behavior of these signals indicates that they correspond to the same His residue. Establishment of NOE connectivity between these signals was prevented by signal overlap, large signal line widths and fast $T_1$ relaxation of the native $Ty_{met}$ $^1$H signals.

That signal *c* shifts downfield shows that the corresponding His residue is not detached upon pnp binding. In that case, an upfield shift toward the diamagnetic region of the spectrum would have been observed.

**2. Titration of Fluoride Bound $Ty_{met}$.** In the absence of pnp, the spectrum of the fluoride bound form of $Ty_{met}$ ($Ty_{met}F$) is much better resolved than the spectrum of native $Ty_{met}$. Six sharp solvent exchangeable signals have been identified before [13] and assigned to the coordinating His-N$^\delta$ protons (labeled *a-f* in Figure 1B), while the remaining broader signals were assigned to the His-C$^\epsilon$ and His-C$^\delta$ protons of the coordinating histidines. Under the experimental conditions (200 mM $F^-$, 4 °C, pH 6.8), $Ty_{met}$ is fully saturated with fluoride ($K_d$ 3 mM [13]), while fluoride itself is in slow exchange on the NMR time scale ($k_{off} < 12$ s$^{-1}$ [14]).

Upon addition of pnp large changes in the paramagnetic $^1$H NMR spectrum of $Ty_{met}F$ are observed, demonstrating the binding of pnp to the $Ty_{met}F$ form. Throughout the spectrum, an increase in [pnp] induces signal shifts and severe line broadening. Since these changes occur gradually with increasing [pnp], the pnp exchange must be intermediate to fast on the NMR time scale.

The large line-broadening observed upon pnp binding and the presence of signal overlap precluded a quantitative analysis of the line widths as a function of [pnp]. Yet, for the majority of signals the amount of signal broadening appears related to the observed shift. For example, signals *c* and *f* shift by a relatively small amount and are still clearly observed at the highest [pnp] used in the titration, while signal *e* already shifts by a substantial amount at low [pnp] and seems to vanish completely upon further increase of [pnp]. This observation is compatible with exchange being the cause for the observed line-broadening. For signal *d* in Figure 1B, no clear shift is observed while its intensity decreases with increasing [pnp]. This can be explained by assuming that this signal shifts by a relatively large amount in comparison to the other signals, causing it to be in slow exchange on the NMR time scale. An exchange contribution to the line-width is confirmed by a marked sharpening of the majority of the signals upon a relatively small increase in temperature (Fig. S1).

**3. Titration of Chloride Bound $Ty_{met}$.** Figure 1C shows selected spectra of $Ty_{met}Cl$ in the absence and in the presence of various amounts of pnp at 4 °C and pH 6.80. The spectra of 0 to 9.0 mM pnp were recorded during a standard titration experiment, while the spectrum containing 18.5 mM pnp was

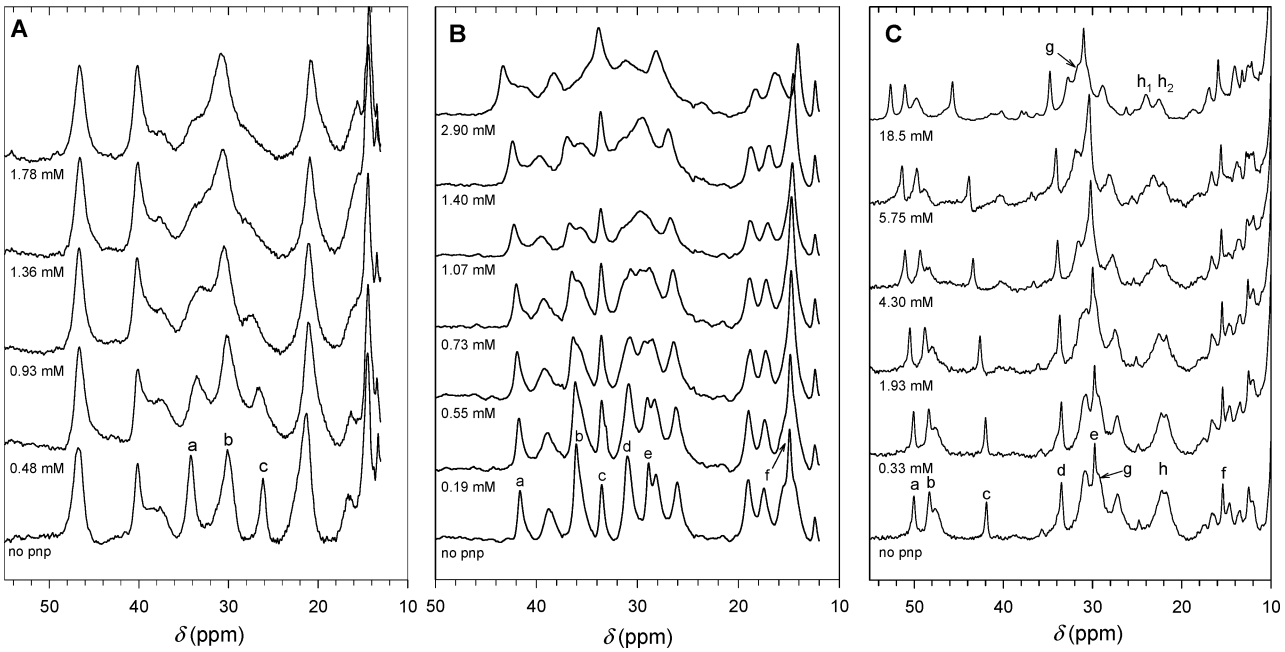


***Figure 1.*** Titrations of (A) native $Ty_{met}$, (B) fluoride bound $Ty_{met}F$ and (C) chloride bound $Ty_{met}Cl$ followed by paramagnetic $^1H$ NMR. Spectra in panels A and C were recorded at 600 MHz resonance frequency while the spectra in panel B were recorded at 300 MHz. In all cases, [Ty] was ~0.7 mM in 100 mM Pi at pH 6.80 at 4 °C. The various [pnp] are indicated under each trace. See text for details and signal labelings.

recorded on a different sample where $Ty_{met}$ was concentrated in a buffer containing 18.5 mM pnp. In contrast with the pnp titrations of native $Ty_{met}$ and $Ty_{met}F$, changes in the paramagnetic $^1H$ spectrum of $Ty_{met}Cl$ appear less drastic, while much higher concentrations of pnp are needed to produce significant changes. Little broadening is detected upon addition of pnp while all signals appear to gradually shift downfield with increasing [pnp], consistent with the pnp ligand being in fast exchange on the NMR time scale.

The absence of large broadening effects allowed us to accurately determine the signal positions of the 6 sharp $N^{\epsilon}H$ signals as a function of [pnp] (Fig. S2). Modest saturation is detected in the data even up to 18.5 mM pnp (close to the pnp solubility limit), indicating that the $K_d$ for the $Ty_{met}Cl$-pnp complex is much higher than the $Ty_{met}Cl$ concentration employed and justifying the use of the simple two-state ligand binding relation given by eq 5

$$\Delta\delta = \Delta\delta_{max}\cdot[pnp]/([pnp]+K_d) \qquad (5)$$

where $\Delta\delta_{max}$ represents the shift for the fully bound $Ty_{met}Cl$-pnp complex. Equation 5 was used to simultaneously fit all shift data where a value for $\Delta\delta_{max}$ was determined for each signal using a single value for the $K_d$. Setting the $K_d$ as a shared parameter between all data sets during the fitting procedure allowed for accurate values to be determined (Table S3).

We also calculated the fractional differences between the $Ty_{met}Cl$ and the estimated $Ty_{met}Cl-pnp$ shifts (assuming a diamagnetic shift of 8 ppm for all signals; Table S3). With the exception of signal *c*, all signals shift downfield by a relatively constant factor of 0.11−0.14 of the original shift upon the binding of pnp. This indicates that the singlet−triplet spacing parameter $-2J$ decreases upon the binding of pnp, causing the fractional population of the paramagnetic $S = 1$ level to increase and, as a consequence, causing the signals to shift farther downfield. The $-2J$ value for $Ty_{met}Cl$ of 200 $cm^{-1}$ [16] corresponds to 17% of spin in the triplet state at 4 °C. To produce an average increase of 12% in shift, the population of the paramagnetic $S = 1$ level has to increase to 19%, corresponding to a $-2J$ value of 150±10 $cm^{-1}$ for the $Ty_{met}Cl-pnp$ ternary complex. A direct measurement of $-2J$ for the ternary $Ty_{met}Cl-pnp$ complex from the temperature dependence of paramagnetic $^1H$ shifts is precluded by the temperature-dependent equilibrium between free and pnp bound $Ty_{met}Cl$ (affecting shifts) and the difficulty that $Ty_{met}Cl$ cannot be saturated with pnp due to the high $K_d$ and limited solubility of pnp. Since both the shifts and the line widths are proportional to the fractional population of the paramagnetic $S = 1$ level, a change in $-2J$ should also be reflected in the line widths. Indeed, for the signal *a*, for which the line width could be determined with reasonable accuracy, a broadening of around 10% is found for the fully bound form.

An exception to the observed trends is signal *c*, which shifts much more (by a fraction of 0.23) upon pnp binding. Since the shift is primarily contact in origin, a substantial change in the contact coupling parameter *A* must occur upon pnp binding. From previous work,[16] it was established that the $N^{\delta}H$ signal *c* shows NOE connectivity to signal *g*, which, therefore, belongs to the same His residue. Due to signal overlap, the position of signal *g* could not be determined precisely as a function of [pnp], but its position could be measured in the absence of pnp (29.26 ppm, see Figure 1C) and in the presence of 18.5 mM pnp (31.72 ppm). By using the experimental $K_d$ value of 18.0 mM and eq 5, it is estimated that $\Delta\delta_{max}$ amounts to 4.85 ppm for signal *g*. Using this value to calculate the fractional increase in shift yields a value of 0.23, i.e., the same value as was found for the corresponding $N^{\delta}H$ signal. Furthermore, signal *h* at 22.27 ppm in the absence of pnp consists of overlapping $C^{\delta}H$ and $C^{\epsilon}H$ signals. Upon addition of pnp, this signal becomes resolved and component $h_1$ shifts to 24.05 ppm in the presence of 18.5 mM pnp. This difference in shift yields a fractional increase of 0.24,

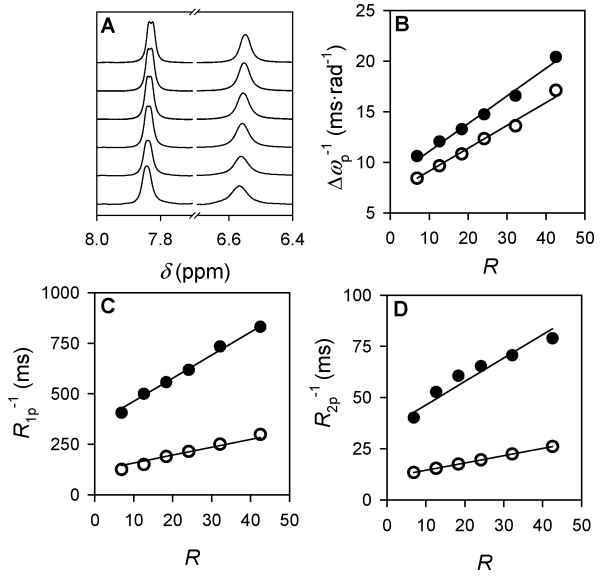


***Figure 2.*** Induced shift and relaxation enhancements of the bulk $^1$H pnp signals as a function of $R$ (= [pnp]/[$Ty_{met}$]) for the native $Ty_{met}$ protein. (A) $^1$H NMR spectra normalized by total peak area with $R = 6.9$ (bottom) to $R = 43$ (top). The pnp ortho protons resonate at ~6.55 ppm, while the meta protons resonate at ~7.85 ppm. Panels B−D show the measured shift differences $\Delta\omega_p^{-1}$, the longitudinal relaxation rate enhancements $T_{1p}$ and the transversal relaxation rate enhancements $T_{2p}$ vs $R$ for the pnp ortho (○) and meta protons (●), respectively. All data in panels B−D were simultaneously fit yielding the parameters denoted in Table 1. Measurements were made in 100 mM Pi at pH 6.80 and 4 °C. $Ty_0$ was 177 $\mu$M.

similar to signals *c* and *g*, suggesting that signal $h_1$ originates from the same His residue. For signal $h_2$ (assigned to a C$^\epsilon$H signal coupled to N$^\epsilon$H signal $e$[16]), a fractional increase in shift of 0.12 is calculated, which puts it in the same class as all the other signals.

Thus, similar to the situation of native $Ty_{met}$, the binding of pnp to $Ty_{met}$Cl apparently causes a change in coordination of one His residue while the remainder of the His residues seem to be less sensitive to the binding of pnp. Using the highest $\Delta\delta_{max}$ value found (signal *c*, 7.9 ppm), and given that pnp is in fast exchange at 600 MHz on the NMR time scale, an upper limit of the exchange time $\tau_M$ can be estimated as $\tau_M < 2 \times 10^{-4}$ s.

**B. NMR of the pnp Signals in the Bulk Solution. 1. Protonated pnp.** The observation that the pnp ligand appears to be in fast exchange with native $Ty_{met}$ on the NMR time-scale, as well as the absence of signals originating from the bound nitrophenol in the paramagnetic $^1$H $Ty_{met}$ spectra (not shown), prompted us to investigate the $^1$H NMR signals of the pnp in the bulk that contain information on the ligand bound to the protein (see Materials and Methods).

The values for the $R_{2p}^{-1}$, $R_{1p}^{-1}$, and $\Delta\omega_p^{-1}$ of the pnp ortho and meta proton signals have been determined as a function of $R$ in 100 mM Pi buffer at pH 6.80 and 279 K by $^1$H NMR titration experiments. Selected spectra recorded in an experiment where a 174 $\mu$M solution of $Ty_{met}$ was titrated with a 18 mM solution of pnp are shown in Figure 2A. In absence of $Ty_{met}$, the 2 equiv ortho protons resonate at 6.53 ppm, while the 2 equiv meta protons give rise to the signal at 7.82 ppm. Apart from the pnp resonances, no other signals become detectable even after prolonged incubation of pnp with large amounts of enzyme, showing that pnp does not react with Ty under the experimental conditions. The presence of $Ty_{met}$ induces broadening of the ortho and meta pnp protons, the broadening of the former being the largest. The experimental values of $R_{1p}^{-1}$, $R_{2p}^{-1}$, and $\Delta\omega_p^{-1}$ as a function of $R$ are presented in Figure 2B−D.

***Table 1.*** pnp Dissociation Constants $K_d$ and Values for $T_{1M}^{app}$, $R_{2M}^{app}$, and $\Delta\omega_p^{app}$ (Expressed as $\delta_M^{app}$ in ppm Units) Determined from the Data Represented in Figure 2[a]

| species | $K_d$ pnp (mM) | pnp protons | $T_{1M}^{app}$ (ms) | $R_{2M}^{app}$ (kHz) | $\delta_M^{app}$ (ppm) |
|---|---|---|---|---|---|
| native $Ty_{met}$ | 7.2 | meta | 8.4 | 1.2 | 1.3 |
| | | ortho | 2.8 | 3.8 | 1.6 |
| $Ty_{met}$F | 6.2 | meta | 8.0 | 1.5 | 1.5 |
| | | ortho | 3.6 | 4.5 | 2.0 |

[a] Standard errors are less than 20% for all parameters.

According to eqs 1−3, $\Delta\omega_p^{-1}$, $R_{2p}^{-1}$, and $R_{1p}^{-1}$ are directly proportional to $f_M^{-1}$, meaning that the dependence of $\Delta\omega_p^{-1}$, $R_{2p}^{-1}$, and $R_{1p}^{-1}$ on $R$ allows for estimation of the dissociation constant $K_d$ and $R_{2M}^{app}$, $R_{1M}^{app}$, and $\Delta\omega_M^{app}$. Accordingly, the data in Figure 2B−D were simultaneously fitted to eqs 1−3 where $K_d$ was set as a global parameter for all datasets. Equal weight was given to all data. Good fits were obtained, in accordance with the binding of a single pnp per $Ty_{met}$ molecule and confirming that the observed changes in $R_{2p}$, $R_{1p}$, and $\Delta\omega_p$ relate to one and the same exchange process. The determined parameters are listed in Table 1 (with $\Delta\omega_M^{app}$ presented as $\Delta\delta_M^{app}$ in ppm).

The titration was repeated for fluoride bound $Ty_{met}$ where 200 mM $F^-$ was present in both the $Ty_{met}$ and pnp stock solutions. The overall behavior was found to be remarkably similar to that observed for native $Ty_{met}$ (not shown). The determined parameters for the $Ty_{met}$F pnp binding are presented in Table 1 and do not differ significantly from the parameters determined for native $Ty_{met}$.

Since the $T_{1M}^{app}$ is a simple function of $\tau_M$ and $T_{1M}$ (eq 3), the different $T_{1M}^{app}$ values determined for the pnp ortho and meta proton signals immediately demonstrate that the exchange contribution to $T_{1p}$ is dominated by the $T_{1M}$ term in eq 3. Thus, the experimental $T_{1M}^{app}$ values closely correspond to the paramagnetic $T_{1M}$ relaxation times of the pnp protons when bound to $Ty_{met}$ and $\tau_M$ must be smaller than the shortest $T_{1M}^{app}$ determined, i.e., $\tau_M < 3{\cdot}10^{-3}$ s, for both native $Ty_{met}$ and $Ty_{met}$F. According to eqs 1 and 2, the $T_{2M}^{app}$ and $\Delta\omega_M^{app}$ are complex functions of $R_{2M}$, $\Delta\omega_M$ and $\tau_M$, each of which is not known explicitly and cannot be solved from the data presented in Figure 2B−D. It is therefore impossible to state whether the calculated values for $R_{2M}^{app}$ and $\delta_M^{app}$ in Table 1 correspond to $R_{2M}$ and $\delta_M$ (i.e., $\Delta\omega_M$) values in eqs 1−3 without further knowledge of the exchange conditions.

**2. Deuterated pnp.** To obtain insight in the exchange conditions, the shift and broadening parameters of the $^2$D signals of completely deuterated pnp were determined as a function of [$Ty_{met}$] (see Materials and Methods). Figure 3A shows selected $^2$D spectra recorded during a titration of deuterated pnp with native $Ty_{met}$ where [pnp] was kept constant at 5 mM throughout the experiment. All spectra were recorded at 4 °C in 100 mM Pi buffer at pH 6.80 at 92.124 MHz resonance frequency.

As in the case of $^1$H pnp, small shifts are observed for both $^2$D signals (Figure 3A). The measured shift is the largest for the pnp ortho protons next to the hydroxyl group. The measured shifts vs [$Ty_{met}$] are plotted in Figure 3C. The data were fit to

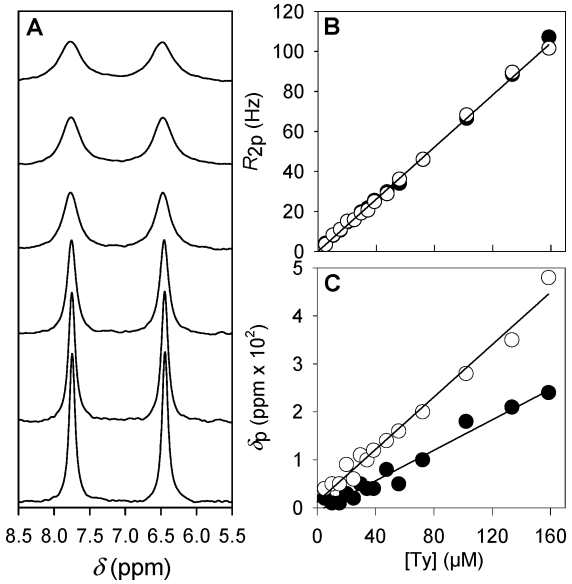


***Figure 3.*** Induced shift and relaxation enhancements of the bulk $^2$D pnp signals as a function of native [$Ty_{met}$]. (A) $^2$D NMR spectra of pnp (5 mM) normalized by total peak area recorded in the presence of increasing amounts of $Ty_{met}$ from 0 (bottom) to 158 $\mu$M (top). Panels B and C show the measured shift differences and the $Ty_{met}$ induced line-broadening vs [$Ty_{met}$] for the pnp ortho (○) and meta protons (●), respectively.

a linear function and from the corresponding slopes and the $K_d$ of 7.2 mM (Table 1), it is estimated that the $\delta_M^{app}$ in the fully $Ty_{met}$ bound form amount to 3.3 and 1.9 ppm for the ortho and meta deuterons, respectively. For the ortho position, the $^2$D $\delta_M^{app}$ is about twice that of the $^1$H $\delta_M^{app}$, while the $^2$D/$^1$H $\delta_M^{app}$ ratio is $\pm$1.5 for the meta position. These relatively small ratios, together with the observation that a larger ratio is measured for the protons with the larger $\delta_M^{app}$, indicate that the pnp is in the fast (for $^2$D) to intermediate (for $^1$H) exchange regime on the NMR time-scale. Thus, the estimated $^2$D $\delta_M^{app}$ of pnp should equal the paramagnetic shifts, $\delta_M$, in the fully bound $Ty_{met}$ form.

With increasing [$Ty_{met}$], severe broadening of the $^2$D signals is observed where the broadening is equal, within the experimental error, for both the pnp ortho and meta deuterons. Line widths were measured by line shape fitting and the resulting $R_{2p}$ values vs [$Ty_{met}$] are represented in Figure 3B. From the slope of a linear fit to the data and the experimental $K_d$ of 7.2 mM, the $R_{2M}^{app}$ values for the $^2$D signals are estimated at 7.9 kHz for both the ortho and meta deuterons. Comparison of this value with the values measured for $^1$H (Table 1) shows that the broadening is larger in the case of $^2$D, meaning that the quadrupolar relaxation significantly contributes to the observed line width. Indeed, with an estimated quadrupolar coupling constant of 193 kHz[31] and a rotational correlation time $\tau_r$ of 15−20 ns,[32] a quadrupolar $R_2$ between 5 and 7 kHz is calculated,[33] which accounts for most of the experimental $^2$D $R_{2M}^{app}$. Factorizing out the quadrupolar relaxation contribution from the observed line widths would require knowledge of the exact value of $\tau_r$ and the quadrupolar coupling constant. From the $^2$D $\delta_M$, the $^1$H $R_{2M}^{app}$, the $^1$H $\delta_M^{app}$ values (Table 1) and eqs 1 and 2, it is now possible to estimate the lifetime of the pnp-$Ty_{met}$ complex $\tau_M$ yielding a value of $2 \times 10^{-4}$ s.

## Discussion

**A. Nitrophenol Does Not Occupy the Cu−X−Cu Bridging Position in $Ty_{met}$F and $Ty_{met}$Cl.** The experiments in which $Ty_{met}$F and $Ty_{met}$Cl were titrated with pnp demonstrate that a ternary $Ty_{met}$−halide−pnp complex is formed. It was previously demonstrated that halides bind at the bridging position between the two Cu(II) ions, replacing the bridging hydroxide in native $Ty_{met}$.[13,14] The pnp must therefore bind at a site other than the bridging position. Furthermore, the values for the dissociation constant $K_d$, as well as the values for the paramagnetic shift and relaxation times of the $Ty_{met}$ bound pnp protons (see below) do not strongly differ between native and fluoride bound $Ty_{met}$. This shows that the presence of fluoride in the active site does not markedly influence the binding of pnp, compatible with different binding sites for fluoride and pnp.

The dissociation constant increases to 18 mM in the case of $Ty_{met}$Cl. Little broadening is detected for the paramagnetically affected signals of $Ty_{met}$Cl upon pnp binding, demonstrating that pnp is in fast exchange on the NMR time scale ($\tau_M < 2 \times 10^{-4}$ s), contrary to the case of $Ty_{met}$F where pnp exchange is slower. Thus, the higher $K_d$ measured for the $Ty_{met}$Cl−pnp complex is at least partly due to a larger pnp off rate, possibly related to steric hindrance by the larger chloride ion.

In previous studies on $Ty_{half-met}$, it was found that a signal assigned to an equatorial hydroxide or water molecule is lost upon pnp binding, while the Cu(II) remains 4-coordinate (3N/1O). It was concluded that the phenolic hydroxyl displaces the hydroxide or water ligand from the paramagnetic Cu(II) ion. The reasons for the different behavior observed in $Ty_{met}$ and $Ty_{half-met}$ are unclear but may reflect, for example, a more spacious active site or a weaker binding of the equatorial $OH^-$/$H_2O$ ligand in $Ty_{half-met}$, rendering this ligand more prone to dissociation.

**B. Binding of pnp Weakens Antiferromagnetic Coupling in $Ty_{met}$Cl.** In $Ty_{met}$Cl, pnp binding causes a decrease in the antiferromagnetic exchange coupling parameter $-2J$ from 200 to 150 cm$^{-1}$, meaning that the two Cu(II) ions become less strongly coupled. Variations in $-2J$ in bridged dinuclear Cu systems have been explained in terms of changes in the Cu-X-Cu bridging angle, smaller angles inducing weaker couplings (e.g., refs 34,35). A correlation between the $-2J$ value and the size of the bridging ion has been observed for the halide complexes of $Ty_{met}$ ($Ty_{met}$F ($-2J$ 260 cm$^{-1}$) > $Ty_{met}$Cl ($-2J$ 200 cm$^{-1}$) > $Ty_{met}$Br ($-2J$ 160 cm$^{-1}$); unpublished results). The lower $-2J$ value for the $Ty_{met}$Cl-pnp complex may therefore reflect a decrease in the Cu−Cl$^-$−Cu bridging angle connected with a decrease in Cu−Cu distance.

For native $Ty_{met}$, there are no systematic upfield or downfield shifts of the paramagnetically shifted signals observed upon pnp binding and no change in $-2J$ had to be invoked to explain the changes in the paramagnetic $^1$H NMR spectra. However, the $-2J$ value of 77 cm$^{-1}$ estimated for the native species[16] is much lower than $k_BT$ (~200 cm$^{-1}$), meaning that the paramagnetic triplet state is close to full population at ambient temperatures. So, a further decrease in $-2J$ will not significantly alter the fractional population of the triplet state and, consequently, the magnitude of the hyperfine shifts.

(31) Ando, M. E.; Gerig, J. T.; Weigand, E. F. *J. Am. Chem. Soc.* **1982**, *104*, 3172−3178.
(32) Cantor, C. R.; Schimmel, P. R. *Biophysical Chemistry, part. II, Techniques for the Study of Biological Structure and Function*; Freeman, W. H.: New York, 1980; pp 539−590.
(33) Sudmeier, J. L.; Anderson, S. E.; Frye, J. S. *Conc. Magn. Reson.* **1990**, *2*, 197−212.

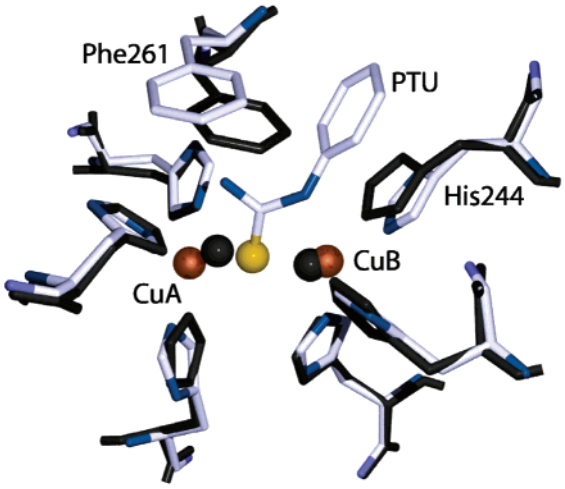


***Figure 4.*** Superposition of the type-3 center of sweet potato catechol oxidase in the native oxidized form (dark gray; PDB entry 1BT1) and with PTU bound (CPK color coding; PDB entry 1BUG). Upon binding of PTU, His244, and Phe261 are displaced while CuB adopts a trigonal bipyrimidal coordination geometry. The position of the PTU aromatic ring is fixed by Phe261. The copper ions and the $Cu_2$ bridging sulfur atom of PTU are shown as spheres (with arbitrary radii). The overlay was generated using the all-atom least-squares superimposition fitting algorithm implemented in the Swiss-PBD Viewer program. Hydrogen atoms of coordinating His residues are omitted for clarity.

**C. Binding of *p*-Nitrophenol Affects Only One His Residue in Native $Ty_{met}$ and $Ty_{met}Cl$.** In the absence of a structural model of Ty, it is customary to use CO[10] and Hc[6−9] structures as models for Ty. An all-atom rmsd minimized superposition of the active sites of $CO_{met}$ (pdb 1BT3) and phenylthiourea (PTU) bound $CO_{met}$ (pdb 1BUG) is depicted in Figure 4. Apart from a larger Cu−Cu distance found in the PTU bound $CO_{met}$, the structures superimpose well and the positions of 5 of the 6 coordinating His residues remain nearly unchanged upon PTU binding. The interaction with CuB however induces a displacement of His244, while the PTU aromatic ring acquires a $\pi-\pi$ interaction with the same His residue. The CuB goes from distorted tetrahedral in the native met form to almost perfectly trigonal bipyramidal in the PTU bound form[10] with His240, His244, and the PTU sulfur atom in the equatorial plane and His274 and the PTU nitrogen atom in the two axial positions.

In our case, it appears that one His residue is particularly sensitive to the binding of pnp in native $Ty_{met}$ and $Ty_{met}Cl$. Thus, signals b and c for native $Ty_{met}$ (Figure 1A) and signals c, g, and $h_1$ for $Ty_{met}Cl$ (Figure 1C) may well correspond to a His similar to His244 in $CO_{met}$.

**D. *p*-Nitrophenol Is Coordinated to the Type-3 Copper.** From the $^1H/^2D$ titration experiments, it was found that the pnp is in fast exchange on the $^2D$ NMR time scale. The shift differences $\delta_M$ between free pnp and pnp in the $Ty_{met}$ bound form amount to 3.3 ppm (ortho) and 1.9 ppm (meta). Since the paramagnetic shifts are dominated by the contact contribution in $Ty_{met}$,[16] the nonzero $\delta_M$ values are consistent with direct coordination of pnp to the metal center.

A comparison of the experimental $\delta_M$ values with the paramagnetic shifts of the coordinating histidines indicates that the contact couplings of the pnp ring protons are weak. This is because the pnp protons are one bond further away from Cu than their His imidazole counterparts. A similar observation has been reported for several small dinuclear $Cu_2$ complexes where the signal shifts of the $Cu_2$ bridging phenolate ring protons are smaller than the shifts of the signals from the coordinating imidazole or pyridyl protons.[18,19,36]

**E. Structural Model of pnp Binding.** The longitudinal relaxation times ($T_{1M}$) for the ortho and meta ring protons of pnp bound to native $Ty_{met}$ and $Ty_{met}F$ (Table 1) do not differ much and will be discussed together. They are dominated by the dipolar contribution,[16] which is proportional to the inverse sixth-power of the distance $r$ between the resonating nucleus and the paramagnetic center. This, in principle, allows for the calculation of H−Cu distances. However, since the paramagnetism is spread over the whole unpaired spin wave function, a quantative evaluation of dipolar $T_1$s requires the integration of the dipolar interaction over the total wave function. The latter is not available. Therefore, a simplified model for the spin distribution allowing for a semiquantitative analysis will be used.

First, it should be noted that the $T_1$ values found for the pnp ortho protons are smaller than for the meta protons, in line with the hydroxylic moiety being oriented toward the active site Cu and the ortho protons being closer to Cu than the meta protons. Furthermore, the experimental $T_{1M}$ values for the pnp ortho protons (Table 1) are similar to those of the His−$C^{\delta}H$ and His−$C^{\epsilon}H$ protons, which are located at ∼3.4 Å from Cu ($T_1$ ∼3 ms[16]) in native $Ty_{met}$ and $Ty_{met}F$. This is compatible with a Cu−H distance of 3−4 Å for the pnp ortho protons, again consistent with pnp coordination to Cu through the phenolic hydroxyl group.

For a semiquantitative analysis, a model is used in which single magnetic point dipoles are placed on the two Cu atoms. Keeping in mind that there are two ortho and two meta protons and that the measured $T_1$s are the averages both for the meta ($T_{1m}$) and for the ortho ($T_{1o}$) protons, the $T_{1m}/T_{1o}$ ratio is given by

$$\frac{T_{1m}}{T_{1o}} = \sum_{i,j} r_{mi-\mathrm{Cu}_j}^{-6} / \sum_{i,j} r_{oi-\mathrm{Cu}_j}^{-6} \qquad (6)$$

with $i,j = 1$ and 2. The experimental $T_{1m}/T_{1o}$ ratios are ∼3 and ∼2 for pnp bound to native $Ty_{met}$ and $Ty_{met}F$, respectively.

As a starting configuration for the semiquantitative analysis, the $CO_{met}$ with bound PTU was taken, in which the PTU was replaced with phenol without adjusting the position of the aromatic ring. Subsequently, the phenol was moved along its long axis until the CuB−O distance amounted to 1.9 Å.[37] The Cu−Cu distance was set at 2.9 Å as in $CO_{met}$. This configuration yields a $T_{1m}/T_{1o}$ ratio of 13 (eq 6), which does not correspond to the experimental ratio of 2−3. The situation could not be improved by allowing the aromatic ring to move in its original plane and/or to rotate around the Ar−O bond. A lower $T_{1m}/T_{1o}$ ratio could only be achieved by allowing the aromatic ring to tilt toward CuA (see Figure 5). The particular structure drawn in Figure 5 does not result in steric clashes with any of the coordinating His residues and has a calculated $T_{1m}/T_{1o}$ ratio of 3.5, which brings it within the bandwidth of the experiment

(34) Komaei, S. A.; van Albada, G. A.; Haasnoot, J. G.; Kooijman, H.; Spek, A. L.; Reedijk, J. *Inorg. Chim. Acta* **1999**, *286*, 24−29.
(35) Rodriguez-Fortea, A.; Alemany, P.; Alvarez, S.; Ruiz, E. *Inorg. Chem.* **2002**, *41*, 3769−3778.
(36) Maekawa, M.; Kitagawa, S.; Munakata, M.; Masuda, H. *Inorg. Chem.* **1989**, *28*, 1904−1909.
(37) Ito, N.; Phillips, S. E.; Stevens, C.; Ogel, Z. B.; McPherson, M. J.; Keen, J. N.; Yadav, K. D.; Knowles, P. F. *Nature* **1991**, *350*, 87−90.

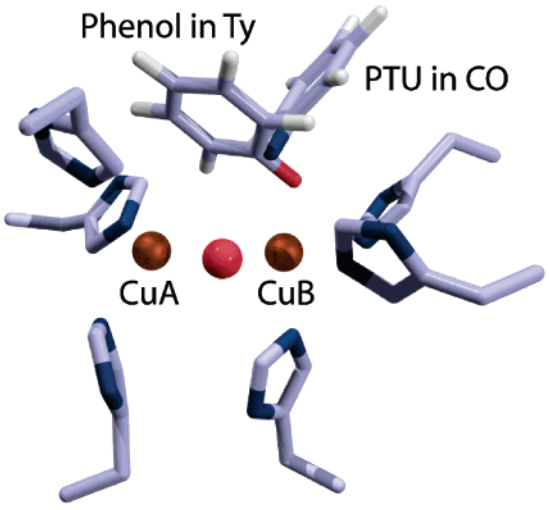


***Figure 5.*** Model of phenol coordination to the oxidized tyrosinase type-3 center. The drawn structure is based on the X-ray structures of oxidized sweet potatoe catechol oxidase (1BT1 and 1PTU) and explains the presented NMR data of pnp binding to $Ty_{met}$ (see text for details). The position of PTU in catechol oxidase is fixed in place by Phe261 (as shown in Figure 4). In Ty, instead, the ortho protons of the bound phenol can approach the $Cu_2$ bridging peroxide present in oxygenated Ty because there is no aromatic residue at the equivalent position in Ty. Both the copper ions and the bridging atom (= $OH^-$, $F^-$, or $Cl^-$) are represented by spheres (with arbitrary radii). Only the aromatic ring and coordinating O or N atom are shown for the bound pnp and PTU, respectively. The hydrogen atoms of coordinating His residues are omitted for clarity.

considering the simplicity of the model used for the calculation. For the drawn configuration, the Cu−O−Ar angle is 114°, which is similar to the Cu−O−Ar angle of 127° for the tyrosine coordinated to Cu in galactose oxidase.[37] We note that this ensures maximum overlap between the oxygen lone pair of the phenolic hydroxyl group and the CuB $d_{z^2}$ orbital (the Cu $d_{x^2-y^2}$ orbitals being oriented in the Cu−X−Cu equatorial plane[25]). Furthermore, the coordination geometry of the phenol in Figure 5 would be compatible with the proposed binding mode of diphenolic substrates in $Ty_{met}$.[13,38,39]

**F. Mechanistic Implications.** While the present study has addressed the binding of monophenols to $Ty_{met}$, the mechanistically relevant complex is that between monophenols and $Ty_{oxy}$. Monophenol binding to $Ty_{met}$ results in a dead-end complex. Still, the present results may be relevant for a better understanding of the interaction of $Ty_{oxy}$ with phenols. It has been observed that the active site His residues in oxidized and oxygenated *Limulus* Hc nearly exactly superimpose (rmsd 0.20 Å). This supports the idea that the positions of the His ligands need not be largely different for the oxy and the met forms of a type-3 Cu center. The recognition of exogenous substrates, therefore, need not differ either between the oxy and met forms.

From spectroscopic evidence it has been concluded that there is a 3 His coordination around each Cu in $Ty_{oxy}$.[40] The current results demonstrate that all six His ligands remain bound to the $Cu_2$ site upon pnp binding to $Ty_{met}$. These results are at variance with suggestions that the Ty active site only contains five His ligands or that a sixth His ligand, if present, detaches from Cu upon phenol binding.[41]

There has been considerable debate regarding the origins of the different activities of Hcs, COs and Tys. It is generally believed that these originate from variations in protein structure that modulate the accessibility of substrates to the type-3 center. For example, in octopus Hc, a capping domain is present that shields the type-3 site from the access of potential substrates. A homologues domain is found in a latent form of CO, which inhibits CO activity.[42] Indeed, proteolytic removal of the capping domain from octopus Hc [43] induces weak phenolase activity, while several Hcs show diphenolase activity upon mild denaturation.[44−46]

To explain the absence of hydroxylase activity in COs, it is been suggested that in Ty phenolic substrates interact with CuA,[11,44,47,48] while diphenolic substrates would interact with CuB. Access to CuA in CO would be blocked by Phe261, leaving CO with diphenolase activity only.[44,48] For *S. antibioticus* Ty, however, experimental data suggest that pnp and bidentate inhibitors both interact with CuB.[38]

The present and previous[38] results are consistent with pnp binding to CuB, where the pnp aromatic ring is tilted toward the noncoordinating CuA as depicted in Figure 5. In this orientation, one of the ortho protons of the phenolic ring would be oriented toward the bound peroxide in $Ty_{oxy}$, a prerequisite for efficient oxygen atom transfer. In contrast, the PTU aromatic ring is tightly held in place by Phe261 in $CO_{met}$, preventing a similar orientation of the aromatic ring and precluding a direct approach of the aromatic ortho protons toward the bound peroxide. An aa sequence alignment of various Hcs, Tys, and COs[1,5,49] shows that a Phe analogous to Phe261 in CO is absent in Tys. We, therefore, suggest that the difference in the monophenolase activity between Ty and CO is due the blocking activity of Phe261 in CO, preventing a direct approach of the substrate to the bound peroxide.

The presented and previous results allow for the proposal of a reaction mechanism as outlined in Scheme 1 (see scheme legend for details), which includes features of previous proposals (e.g., refs 11,23,47). The modifications include the following: (1) phenol coordinates to CuB in an orientation allowing for oxygen transfer to the phenolic ortho position; (2) the diphenol coordinates to CuB in $Ty_{met}$, where one of the phenolic oxygens bridges the two Cu ions;[13,38,39] (3) proton transfer from a phenolic hydroxyl to the $Cu_2$ bridging $OH^-$ ion assists in diphenol binding to $Ty_{met}$;[14] and (4) a second base assists in the deprotonation of both monophenolic and diphenolic substrates.[44,48]

In the proposed reaction scheme, the total charge of the complex cycles between +3 and +2 during all stages of the mechanism, which limits both destabilizing fluctuations in net charge and in the flux of protons from and to the $Cu_2$ center. From the structure of CO and from sequence homology, a role for proton uptake has been suggested for a conserved Glu residue that is present in the CuB site of most COs and Tys.[50]

(38) Bubacco, L.; Van Gastel, M.; Groenen, E. J.; Vijgenboom, E.; Canters, G. W. *J. Biol. Chem.* **2003**, *278*, 7381−7389.
(39) Van Gastel, M.; Bubacco, L.; Groenen, E. J.; Vijgenboom, E.; Canters, G. W. *FEBS Lett.* **2000**, *474*, 228−232.
(40) Longa, S. D.; Ascone, I.; Bianconi, A.; Bonfigli, A.; Castellano, A. C.; Zarivi, O.; Miranda, M. *J. Biol. Chem.* **1996**, *271*, 21025−21030.
(41) Siegbahn, P. E. *J. Biol. Inorg. Chem.* **2003**, *8*, 567−576.
(42) Gerdemann, C.; Eicken, C.; Galla, H. J.; Krebs, B. *J. Inorg. Biochem.* **2002**, *89*, 155−158.
(43) Salvato, B.; Santamaria, M.; Beltramini, M.; Alzuet, G.; Casella, L. *Biochemistry* **1998**, *37*, 14065−14077.
(44) Decker, H.; Tuczek, F. *Trends Biochem. Sci.* **2000**, *25*, 392−397.
(45) Decker, H.; Ryan, M.; Jaenicke, E.; Terwilliger, N. *J. Biol. Chem.* **2001**, *276*, 17796−17799.
(46) Decker, H.; Rimke, T. *J. Biol. Chem.* **1998**, *273*, 25889−25892.
(47) Olivares, C.; Garcia-Borron, J. C.; Solano, F. *Biochemistry* **2002**, *41*, 679−686.

***Scheme 1.*** Schematic Representation of the Ty Reaction Mechanism[a]

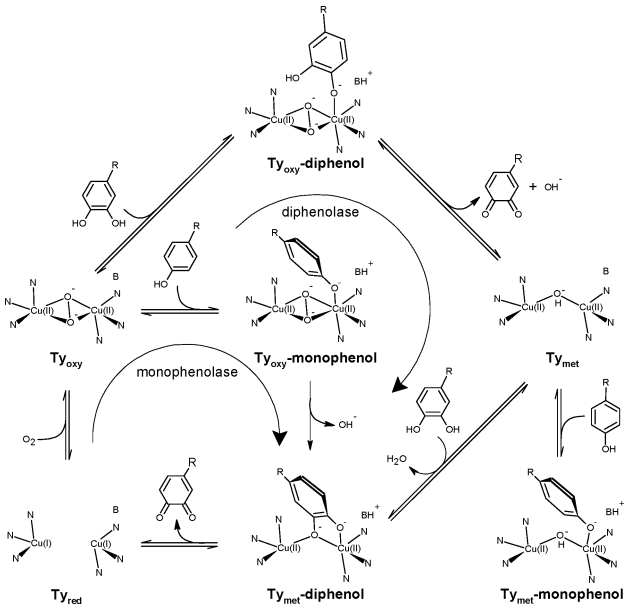


[a] The monophenolase pathway starts with the binding of $O_2$ to $Ty_{red}$ to render $Ty_{oxy}$. phenolic substrate then binds to CuB of $Ty_{oxy}$, where the aromatic ring is oriented toward the bound peroxide. During binding, the phenol transfers a proton to a base B, promoting charge transfer from the phenolic oxygen to $Cu_2$, weakening the O−O bond and poising one of the $O_2^{2-}$ oxygens for electrophilic attack on the phenolic ortho position. After oxygen transfer, the diphenolic product is bound to CuB where one phenolic oxygen bridges the Cu(II) ions.[13,38,39] Diphenol may dissociate from this complex, leaving $Ty_{met}$, or may be oxidized further rendering the quinone product and $Ty_{red}$. The diphenolase pathway involves the oxidation of two diphenol molecules by $Ty_{oxy}$ and $Ty_{met}$ subsequently.[50]

In this regard, we add that in all Tys and COs a conserved noncoordinating His residue is present that is sequentially positioned directly adjacent to a His residue coordinating equatorially to CuB (His274 in sweet potato CO) making this residue another possible candidate as the proton acceptor. The imidazole ring of this (buried) His residue is in direct contact with the imidazole group of His244 that interacts with the bound substrate in CO.

## Summary and Conclusion

We have presented a paramagnetic NMR study of the interaction between the monophenolic inhibitor *p*-nitrophenol (pnp) and the oxidized form of *Streptomyces antibioticus* tyrosinase (Ty) in its native and halide bound forms. The study was aimed at providing insight into the binding mode of monophenolic substrates and has implications toward the understanding of the Ty hydroxylase mechanism and the structural principles underlying the different activities observed for Hcs, COs and Tys.

We find that the pnp forms a ternary complex with halide ($F^-$, $Cl^-$) bound $Ty_{met}$, showing that the pnp phenolic oxygen does not take up the $Cu_2$ bridging position. Furthermore, the experimental pnp $K_d$ values as well as the shifts and the relaxation parameters of the pnp protons bound to native do not significantly differ between $Ty_{met}$ and $Ty_{met}F$ (Table 1). Thus, the presence of $Cu_2$ bridging fluoride does not notably influence the binding of pnp. Additionally, the pnp is shown to directly coordinate to Cu, while the typical $(Cu-His_3)_2$ coordination is maintained upon pnp binding. The pnp, therefore, must be bound to an open coordination position of one of the Cu ions. This is in agreement with earlier proposals for the Ty hydroxylation chemistry (e.g., ref 11) and the binding mode of phenylthiourea in the X-ray structure of CO.[10]

The pnp is in fast exchange with $Ty_{met}Cl$ on the NMR time scale. The titration data of pnp binding to $Ty_{met}Cl$ (Figure 1C) are explained by a decrease in the antiferromagnetic coupling parameter $-2J$ upon pnp binding, indicating an decrease in the Cu−$Cl^-$−Cu bridging angle and the Cu−Cu distance. If a similar situation applies to the binding of monophenol to $Ty_{oxy}$, it may influence the reactivity of the bound peroxide. Furthermore, the binding of pnp to native $Ty_{met}$ and $Ty_{met}Cl$ affects one His residue in the $(Cu-His_3)_2$ coordination sphere, which is tentatively assigned to the Ty analogue of His244 that interacts with the PTU inhibitor in $CO_{met}$.

The exchange of pnp between the free and the $Ty_{met}$ bound forms allowed for the measurement of the $T_1$ values of the pnp ring protons bound to $Ty_{met}$ and $Ty_{met}F$ (Table 1). From this, we were able to deduce a structural model for phenol coordination to $Ty_{met}$ (Figure 5). In this model, the phenol is axially coordinated to CuB with its aromatic ring tilted toward CuA. In the delineated orientation, the ortho protons of the bound phenol are oriented toward the bound peroxide in $Ty_{oxy}$, allowing for the hydroxylation of the phenol. In CO, instead, a similar orientation of phenol is prevented by Phe261 that shields the active site and locks the bound substrate in its place (Figure 4), thereby explaining the absence of hydroxylase activity in CO.

**Acknowledgment.** This research was supported by the Dutch Science Foundation NWO (Project no. 700-28-047). We thank Cees Erkelens and Ursula Kolczak for help with the NMR measurements.

**Supporting Information Available:** Temperature dependence of the paramagnetic $^1H$ NMR spectrum of the $Ty_{met}F$−pnp complex; Paramagnetic shift differences $\Delta\delta$ vs [pnp] for the 6 sharp $Ty_{met}Cl$ $N^{\delta}H$ signals measured during a titration of $Ty_{met}$-Cl with pnp; Shift differences ($\Delta\delta_{max}$) of the $^1H$ $N^{\delta}H$ signals between $Ty_{met}Cl$ and the $Ty_{met}Cl$−pnp ternary complex. This material is available free of charge via the Internet at http://pubs.acs.org.

JA0454687

(48) Decker, H.; Dillinger, R.; Tuczek, F. *Angew. Chem., Int. Ed.* **2000**, *39*, 1591−1595.
(49) Gerdemann, C.; Eicken, C.; Krebs, B. *Acc. Chem. Res.* **2002**, *35*, 183−191.
(50) Eicken, C.; Krebs, B.; Sacchettini, J. C. *Curr. Opin. Struct. Biol.* **1999**, *9*, 677−683.